

Low-threshold stimulated emission from lysozyme amyloid fibrils doped with a blue laser dye

L. Sznitko, P. Hanczyc, J. Mysliwiec, and M. Samoc

Citation: [Applied Physics Letters](#) **106**, 023702 (2015); doi: 10.1063/1.4905782

View online: <http://dx.doi.org/10.1063/1.4905782>

View Table of Contents: <http://scitation.aip.org/content/aip/journal/apl/106/2?ver=pdfcov>

Published by the [AIP Publishing](#)

Articles you may be interested in

[Stretching of DNA confined in nanochannels with charged walls](#)

Biomicrofluidics **8**, 064121 (2014); 10.1063/1.4904008

[Probing transient protein-mediated DNA linkages using nanoconfinement](#)

Biomicrofluidics **8**, 034113 (2014); 10.1063/1.4882775

[Facile fabrication processes for hydrogel-based microfluidic devices made of natural biopolymers](#)

Biomicrofluidics **8**, 024115 (2014); 10.1063/1.4871936

[Structural fingerprints and their evolution during oligomeric vs. oligomer-free amyloid fibril growth](#)

J. Chem. Phys. **139**, 121901 (2013); 10.1063/1.4811343

[Study of dye molecule orientation and configuration in dye molecule doped polythiophene films](#)

J. Vac. Sci. Technol. A **25**, 1547 (2007); 10.1116/1.2784722



HIDEN ANALYTICAL Instruments for Advanced Science

| | | | |
|--|---|---|---|
|  <p>Gas Analysis</p> <ul style="list-style-type: none">dynamic measurement of reaction gas streamscatalysis and thermal analysismolecular beam studiesdissolved species probesfermentation, environmental and ecological studies |  <p>Surface Science</p> <ul style="list-style-type: none">UHV TPDSIMSend point detection in ion beam etchelemental imaging - surface mapping |  <p>Plasma Diagnostics</p> <ul style="list-style-type: none">plasma source characterizationetch and deposition process reactionkinetic studiesanalysis of neutral and radical species |  <p>Vacuum Analysis</p> <ul style="list-style-type: none">partial pressure measurement and control of process gasesreactive sputter process controlvacuum diagnosticsvacuum coating process monitoring |
|--|---|---|---|

Contact Hiden Analytical for further details:
W www.HidenAnalytical.com
E info@hiden.co.uk
CLICK TO VIEW our product catalogue

Low-threshold stimulated emission from lysozyme amyloid fibrils doped with a blue laser dye

L. Sznitko,^{a),b)} P. Hanczyc,^{b),c)} J. Mysliwiec, and M. Samoc

Advanced Materials Engineering and Modelling Group, Faculty of Chemistry, Wrocław University of Technology, Wrocław 50-370, Poland

(Received 3 December 2014; accepted 26 December 2014; published online 13 January 2015)

Amyloid fibrils are excellent self-assembling nanotemplates for organic molecules such as dyes. Here, we demonstrate that laser dye-doped lysozyme type fibrils exhibit significantly reduced threshold for stimulated emission compared to that observed in usual matrices. Laser action was studied in slab planar waveguides of the amyloids doped with Stilbene 420 laser dye prepared using a film casting technique. The lowering of the threshold of stimulated emission is analyzed in the context of intrinsic structure of the amyloid nanotemplates, electrostatic interaction of different microstructures with dye molecules, as well as material properties of the cast layers. All these factors are considered to be of importance for introducing gain for random laser operation. © 2015 AIP Publishing LLC. [<http://dx.doi.org/10.1063/1.4905782>]

Proteins are a large and very diverse class of complex organic chemical compounds that are essential for living organisms.¹ Their distinct and varied three-dimensional structures are composed of one or more long chains of amino acids connected by peptide bonds, typically forming α -helices and β -sheets, as well as looping and folded chains.² Distinguishing microstructures can be found in amyloid fibrils, the aggregated state proteins that are considered to be involved in serious neurodegenerative diseases such as Alzheimer's,³ Parkinson's,⁴ or Huntington's.⁵ Generally, amyloid fibrils are composed of antiparallel β -sheets oriented perpendicular to the long-axis of the fibril, which can be as long as several micrometres but with a diameter of only some 8–10 nm.⁶ In the case of lysozyme fibrils, mixed unstructured regions can appear, such as α -helices⁷ or random coils,⁸ which may co-exist in equilibrium with the β -sheets.

Amyloid fibrils are attracting much attention not only because of their biological relevance but also because of their unique and unusual material properties as self-assembling nanotemplates exhibiting, e.g., the pull strength comparable to steel, mechanical shear stiffness similar to that of silk, and extreme persistence length and mechanical rigidity.⁹ Recently, we reported on surprisingly strong multiphoton interaction of femtosecond laser light pulses with amyloid fibrils.¹⁰ The fact that the fibrillization process can be induced in laboratory conditions in almost any type of protein makes amyloid-based structures interesting nanomaterials for a broad spectrum of technological applications spanning from biophotonics¹⁰ to bottom-up designed optoelectronic devices.¹¹

An important issue for detecting specific types and structures present in amyloid fibrils by optical means, relevant for diagnostics of neurodegenerative diseases, is finding specific staining agents capable of being sensed at high signal-to-noise ratio. In this article, we present results of studies performed on lysozyme-type amyloids doped with

the Stilbene 420 laser dye, whose emission in the bound state is found to exhibit features that appear to be related to the intrinsic microstructure of the fibrils. We conclude that the ordering of chromophores achieved using the amyloid fibril nanotemplates leads to a biologically derived lasing medium showing remarkably lowered amplified spontaneous emission (ASE) threshold.

Binding of Stilbene 420 molecules to the amyloid structures was proven by Linear Dichroism (LD) spectra measurements. LD of amyloid-dye complexes flow-oriented in solution can provide general information if the dye molecule is capable of binding to amyloid fibrils. The geometry of the bound chromophore relative to the tyrosine position in fibrils protofilaments can then be determined according to Ref. 12. In the present case, the LD spectra contain a strong positive band around 360 nm, as shown in Fig. 1(a), which is an indication of the binding. This is likely to be the result of the negatively charged $-\text{SO}_3^-$ groups of Stilbene 420 dye molecules interacting electrostatically with positively charged amino acid residues of the amyloids which leads to the dye molecules becoming spatially organized (Fig. 1(b)). Calculating the reduced linear dichroism LD^r (Ref. 12) and taking $S = 0.08$ as the orientation factor of fibrils¹³ allows to estimate the average binding angle of Stilbene 420 molecules with respect to the fibril axis as 20° . This value indicates that the long axis of the dye essentially lies along the fibril structure. The geometry is thus similar to that proposed for other amyloid staining agents including the most common ones, Thioflavin T (Ref. 14) and Congo Red.¹⁵

Stimulated emission was investigated on solid samples of the amyloid-dye adduct¹² that were solution cast on silica plates and left to dry. The samples were illuminated with $\lambda = 355$ nm nanosecond pulses using the third harmonic of a Nd:YAG laser.¹² This wavelength fits well to the absorption maximum of Stilbene 420 [Fig. 1, blue solid line].

The emission was recorded at various spots of the layers, which appeared to contain different morphology microdomains formed upon drying, as evident from fluorescence microscopy images shown in Fig. 2. Typically, three types of

^{a)}E-mail: lech.sznitko@pwr.edu.pl

^{b)}L. Sznitko and P. Hanczyc contributed equally to this work.

^{c)}E-mail: piotr.hanczyc@pwr.edu.pl

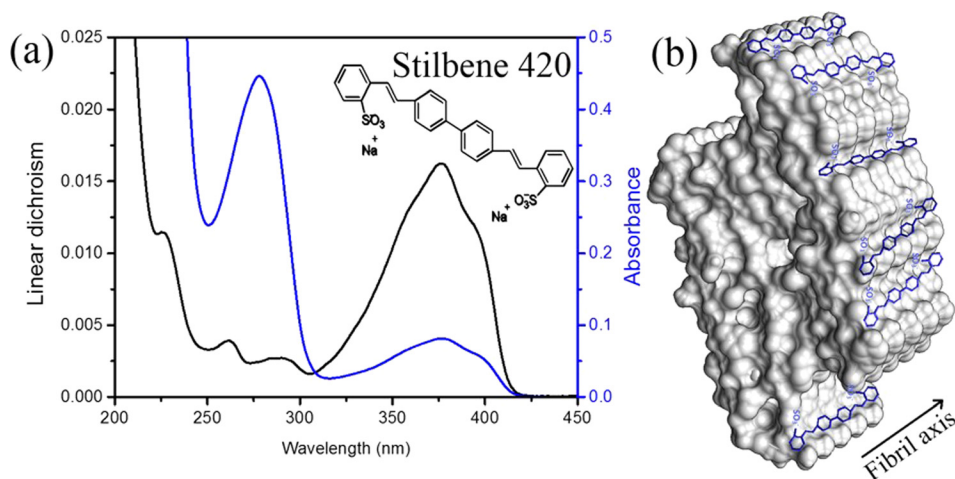


FIG. 1. LD spectrum (black line) of amyloid-Stilbene 420 adduct in pH = 2 buffer and normalized absorbance (blue line). The inset presents molecular structure of the dye (a). Schematic illustration of the dye binding to the amyloid fibril (b).

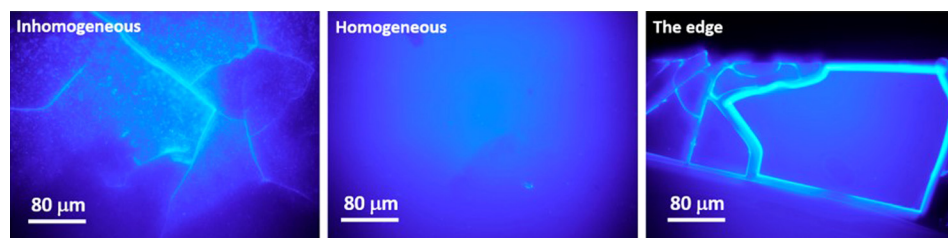


FIG. 2. Comparison of fluorescence microscope images showing three different spots on the amyloid-Stilbene 420 layer. The regions are denoted as inhomogeneous, homogeneous, and the edge.

surface morphology could be discerned in the layers. Briefly, the central region of the cast film, denoted as “inhomogeneous” in Fig. 2, contained defects and had low optical transparency. The defects could be due to the crystallization of non-fibrillized proteins and/or the dye. The surrounding area, denoted as “homogeneous,” was optically transparent, with no defects visible. The edges of the sample had multiple cracks where enhanced emission could be seen. Fluorescence images presented in Fig. 2 show examples of mentioned sample regions.

The emission recorded in regions denoted as inhomogeneous showed no indications of ASE behaviour. The scattering point defects seen in the microscope images could be in fact aggregates of phase-separated dye molecules, since a similar pattern could be seen for the dye itself cast on glass from solution.¹² We cannot also rule out the presence of trace amounts of non-fibrillized proteins present in the inhomogeneous region as a side effect in preparation protocol of the fibrils. It needs to be remarked that, as indicated by our results, Stilbene 420 does not interact with native lysozyme protein and binds exclusively to amyloid fibrils.¹²

In contrast to the inhomogeneous regions, in which light amplification was apparently made not plausible by excess losses and lasing did not occur, measurements performed in the homogeneous regions and at the edges of the layers exhibited distinct spectral narrowing of the emission upon reaching a certain threshold level, which is typical for processes based on stimulated emission, like ASE or random lasing (RL).^{16–18} Comparing stimulated emission spectra and fluorescence of the bound Stilbene 420 [Fig. 3] one can observe coinciding of the stimulated emission peak with one of the vibrational modes seen in the fluorescence, which indicates that the emission occurs in this mode with the highest efficiency. Knowing that the vibrational spectrum of stilbene depends on the

molecule planarity as well as surrounding local environment¹⁹ one may suggest that interactions with specific microstructures in amyloids (β -sheet, α -helix, random coil, etc.) are crucial for inducing stimulated emission in the amyloid-dye adduct. It is plausible that some binding geometries are favoured to induce stimulated emission, analogically to DNA systems where intercalation between the nucleobases is suggested to be most favourable to achieve light amplification.^{17,20}

The emission intensity dependence on the pumping energy density is presented in log-log scale as inset in Fig. 3. The stimulated emission occurs above the threshold level of pumping, which can be observed as spectrum narrowing and increase of intensity. In the case of probing the homogeneous

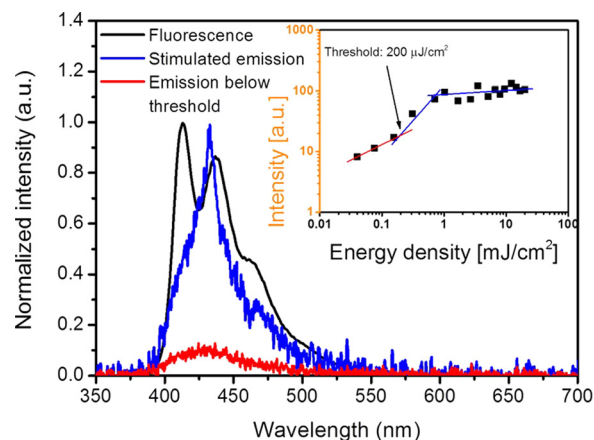


FIG. 3. Comparison of emission spectra obtained for lysozyme fibrils doped with Stilbene 420 laser dye. Black line is for liquid sample in water buffer (pH = 2), blue line is for stimulated emission coming from solid thin film, and red line is for emission from solid thin film below threshold of stimulated emission. Inset shows the dependence of the emission intensity on fluence of the pumping light in log-log scale.

area of the film, the value of the threshold was estimated to be around $\rho_{th} \approx 200 \mu\text{J}/\text{cm}^2$, which is an order of magnitude lower than typical values for chromophores incorporated in polymer matrices²¹ and the same magnitude as the value reported for silk fibroin.²² However, the most striking effect was observed when probing the edge area that contained cracks [Fig. 2(c)]. The stimulated emission threshold was found to be significantly reduced in that case and its value was as low as $\rho_{th} = 70 \mu\text{J}/\text{cm}^2$, depending on the number and size of cracks [see the inset in Fig. 4(a)]. This is the one of the lowest values recorded for any biologically derived material used for lasing experiments. The mechanism behind it can be explained by positive feedback, reducing the stimulated emission threshold that could be introduced to the system through the numerous defects like those shown in Fig. 4(b).¹⁸ The cracks of certain size can play the same role as tightly packed grains of laser material in powder lasers.²³ The emission spectra are in the present case narrower. The full width at half maximum for the emission excited with energy density $\rho = 1 \text{ mJ}/\text{cm}^2$ was reduced from 27 nm to 4 nm, which was the resolution limit of the used spectrometer. In order to investigate how surface defects influence the emitted light, a CCD camera and a microscope objective were placed in front of the amyloid-dye layer in such a way that the illuminated area was imaged on the CCD array with $5\times$ magnification (the excitation beam was incident at 30° with respect to the surface normal to prevent direct exposure of the CCD camera sensor to the beam).

The obtained images confirmed the contribution of cracks to the feedback. This type of defects is responsible for multiple light scattering which gives rise to diffusive-like propagation of light in the sample plane. Such propagation creates positive, but incoherent, feedback for the stimulated emission, thus, the observed emission spectra are rather “smooth,” without evidence of narrow emission lines typical for coherent random lasing. Random lasing emission type (coherent or incoherent) is strongly dependent on experimental conditions. In our case, the illuminated area had a circular shape with diameter of 3 mm which covered whole microscopic images as shown in Fig. 4(b). The circular shape of that area together with planar waveguide design of the sample creates a quasi, two-dimensional system for amplified light propagation. Top and middle pictures show the same part of the layer edge excited below and above the threshold

level, respectively. A brighter region highlighted with a white ellipsoid indicates the region where the lasing occurs. The emergence of this bright region coincided with the appearance of the lasing peak in the emission spectra, thus it can be interpreted as the region where the interplay between gain and disorder satisfies conditions for random lasing. Bright spots that appear at the edges of crack when the threshold level is reached are an evidence of the scattering of emitted light taking place at this type of defects. The microscopic picture presented in the bottom of Fig. 4(b) shows a region where the number of defects was higher (and had the lowest observed threshold) thus the average distance between them was smaller. This leads to shortening of the mean free photon path and thus more effective scattering. The region, where the laser light is generated, is then much more expanded in this case and directly indicates that number of defects, their size, and relative position determines the lasing performance. The average distance between scattering for the situation depicted in Fig. 4(b) in the top and in the bottom pictures is around 109 and $43 \mu\text{m}$, respectively. A possible explanation of the emergence of cracks at the edges of the sample can be related to the mechanical properties of amyloid fibrils. High rigidity leads to spontaneous breaking of long fibril filaments ($\sim 10 \mu\text{m}$) within time regime of minutes in solution.⁹ In the case of solvent evaporation, the breaking process can be accelerated by internal stress, in the fashion similar to organic polymers that form crack defects during layer formation.²⁴

In conclusion, we have shown that self-assembling amyloid fibrils are excellent nanotemplates for organizing chromophores, as shown on the example of Stilbene 420. Molecular interactions with the bio-derived matrix can improve the emission efficiency compared to that of organic polymer systems (poly(vinyl) alcohol, poly(methyl methacrylate), etc.) doped with dyes, because the chromophores are equally distributed over the binding sites and no dye aggregation appears. This allows for higher local concentrations of the chromophores in the nanotemplate and for shortening the distances between the bound molecules.

The data shown here indicate that the threshold for stimulated emission in chromophore-doped amyloids is exceptionally low and can be further lowered, especially when random feedback is introduced. This strategy may be particularly promising for a scenario of using non-toxic

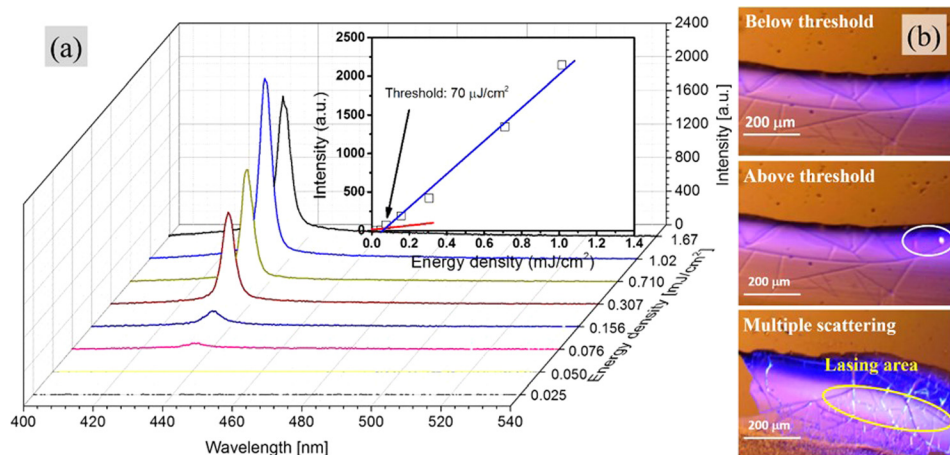


FIG. 4. Stimulated emission spectra of amyloids-Stilbene 420 layer containing cracks (a). Inset shows the dependence of emission intensity on the pumping energy density. Microscopic images of the cast layer showing fluorescence of Stilbene 420 bound to amyloid fibrils below and above the threshold of stimulated emission (b).

histological chromophores for staining disease related fibrils. However, it will be crucial to determine how the stimulated emission is influenced by specific amyloid microstructures and the particulars of binding of the dye molecules to them. On the other hand, materials based on dye-amyloid systems might be promising for more efficient solid state laser devices if their lasing threshold can be further significantly reduced using more controllable mechanisms of feedback, like the distributed feedback (DFB) or distributed Bragg reflection (DBR). Moreover, intentional introduction of specific structures in the amyloid layers could be used in order to fabricate well-defined and high quality and performance micro-laser systems. Thus, the discovery that chromophores bound to amyloid fibrils show efficient lasing may have both medical and technological significance.

We acknowledge funding from the Polish National Science Centre (Grant Nos. DEC-2013/09/D/ST4/03780 and DEC-2013/10/A/ST4/00114), the Foundation for Polish Science (MISTRZ program) and Wroclaw University of Technology. P.H. thanks Catherine Kitts for introduction into the amyloid-dye field.

- ¹T. E. Creighton, *Proteins: Structures and Molecular Properties* (W. H. Freeman and Company, 1993).
²P. E. Wright and H. J. Dyson, *J. Mol. Biol.* **293**(2), 321 (1999).
³J. X. Lu, W. Qiang, W. M. Yau, C. D. Schwieters, S. C. Meredith, and R. Tycko, *Cell* **154**, 1257 (2013).
⁴G. Comellas, L. R. Lemkau, A. J. Nieuwkoop, K. D. Kloepper, D. T. Lador, R. Ebisu, W. S. Woods, A. S. Lipton, J. M. George, and C. M. Rienstra, *J. Mol. Biol.* **411**(4), 881 (2011).
⁵R. Truant, R. S. Atwal, C. Desmond, L. Munsie, and T. Tran, *FEBS J.* **275**(17), 4252 (2008).

- ⁶J. L. Jimenez, E. J. Nettleton, M. Bouchard, C. V. Robison, and C. M. Dobson, *Proc. Natl. Acad. Sci. U.S.A.* **99**(14), 9196 (2002).
⁷I. K. Lednev, *Biological Applications of Ultraviolet Raman Spectroscopy* (Nova Science Publishers, Inc., 2007), Chap. I, p. 16.
⁸Y. Tokunaga, Y. Sakakibara, Y. Kamada, K.-i. Watanabe, and Y. Sugimoto, *Int. J. Biol. Sci.* **9**(2), 219 (2013).
⁹J. F. Smith, T. P. J. Knowles, C. M. Dobson, C. E. MacPhee, and M. E. Welland, *Proc. Natl. Acad. Sci. U.S.A.* **103**, 15806 (2006).
¹⁰P. Hanczyc, M. Samoc, and B. Norden, *Nat. Photonics* **7**(12), 969 (2013).
¹¹M. Hamedi, A. Herland, R. H. Karlsson, and O. Ingenas, *Nano Lett.* **8**(6), 1736 (2008).
¹²See supplementary material at <http://dx.doi.org/10.1063/1.4905782> for sample preparation, calculations of linear dichroism, experimental details, supporting spectroscopic data and microscopic image of Stilbene 420 dye in solid state.
¹³C. Kitts, T. Beke-Somfai, and B. Norden, *Biochemistry* **50**(17), 3451 (2011).
¹⁴A. K. Buell, E. K. Esbjörner, P. J. Riss, D. A. White, F. I. Aigbirhio, G. Toth, M. E. Welland, Ch. M. Dobson, and T. P. J. Knowles, *Phys. Chem. Chem. Phys.* **13**, 20044 (2011).
¹⁵A. K. Schütz, A. Soragni, S. Hornemann, A. Aguzzi, M. Ernst, A. Böckmann, and B. H. Meier, *Angew. Chem. Int. Ed.* **50**(26), 5956 (2011).
¹⁶A. Costela, O. Garcia, L. Cerdan, I. Garcia-Moreno, and R. Sastre, *Opt. Express* **16**(10), 7023 (2008).
¹⁷P. D. Garcia, M. Ibisate, R. Sapienza, D. S. Wiersma, and C. Lopez, *Phys. Rev. A* **80**(1), 013833 (2009).
¹⁸H. Cao, *Waves in Random Media* **13**(3), R1 (2003); A. A. Costela, L. Cerdan, and I. Garcia-Moreno, *Prog. Quantum Electron.* **37**(6), 348 (2013).
¹⁹K. J. Smit and K. P. Ghiggino, *Dyes Pigm.* **8**, 83 (1987).
²⁰W. Lee and X. Fan, *Anal. Chem.* **84**(21), 9558 (2012).
²¹K. Yamashita, M. Arimatsu, M. Takayama, K. Oe, and H. Yanagi, *Appl. Phys. Lett.* **92**, 243306 (2008).
²²S. Toffanin, S. Kim, S. Cavallini, M. Natali, V. Benfenati, J. J. Amsden, D. L. Kaplan, R. Zamboni, M. Muccini, and F. G. Omenetto, *Appl. Phys. Lett.* **101**, 091110 (2012).
²³M. Bahoura and M. A. Noginov, *J. Opt. Soc. Am. B* **20**, 2389 (2003).
²⁴G. C. Costa, A. Z. Simões, G. Gasparotto, M. A. Zaghette, B. Stojanovic, M. Cilense, and J. A. Varela, *Mater. Res.* **6**(3), 347 (2003).